

# High-resolution x-ray diffraction strain–stress analysis of GaN/sapphire heterostructures

V S Harutyunyan<sup>1</sup>, A P Aivazyan<sup>1</sup>, E R Weber<sup>2</sup>, Y Kim<sup>2</sup>, Y Park<sup>2</sup>  
and S G Subramanya<sup>2</sup>

<sup>1</sup> Department of Solid State Physics, Yerevan State University, A Manukian 1, 375049 Yerevan, Armenia

<sup>2</sup> Department of Materials Science and Mineral Engineering, University of California at Berkeley and Materials Science Division, LBN Laboratory, Berkeley, California 94720, USA

E-mail: vharut@server.physdep.r.am

Received 13 September 2000

## Abstract

On the basis of high-resolution x-ray diffraction measurements, the strain–stress analysis of GaN/(00.1) $\alpha$ -Al<sub>2</sub>O<sub>3</sub> heteroepitaxial structures grown by molecular beam epitaxy is performed. The deformation state of the heteroepitaxial structures is investigated depending on the relative content of N in the Ga<sub>1-x</sub>N<sub>x</sub> buffer layer with the given thickness (= 4 nm) and growth conditions. Using the extrapolating technique, the *a*- and *c*-lattice parameters, as well as the in-plane and out-of-plane strains (of the order of  $-10^{-3}$  and  $10^{-4}$ , respectively) are determined for GaN epilayers from  $\theta - 2\theta$  x-ray diffraction spectra. For GaN epilayers, both the biaxial in-plane and in-depth strains (of the order of  $-10^{-3}$  and  $10^{-3}$ , respectively) and the hydrostatic strain component (of the order of  $-10^{-4}$ ) are extracted from the measured strains. It is supposed that the hydrostatic strain in the epilayers is caused by native point defects. The maximal level for the biaxial stress in the GaN epilayer,  $-1.3$  GPa, is achieved for the sample with a relative content,  $x = 0.377$ , of N in the Ga<sub>1-x</sub>N<sub>x</sub> buffer layer.

## 1. Introduction

In recent years, gallium nitride has attracted growing scientific and industrial interest [1]. It is a wide bandgap (3.4 eV at room temperature) compound semiconductor for both optoelectronic and electronic applications, such as bright UV and visible light-emitting diodes, power devices and lasers [2–4]. Since bulk GaN substrates are not readily available, the material is usually grown heteroepitaxially on sapphire [1] ( $\alpha$ -Al<sub>2</sub>O<sub>3</sub>) or 6H-SiC [5] substrates. At present, it is still difficult to obtain a high-quality GaN epilayer both because of the large lattice mismatch (close to  $-14\%$ ) and the difference in the thermal expansion coefficients (close to  $80\%$ ) between the GaN film and the sapphire substrate. This large difference between the lattice parameters and the thermal expansion coefficients between the film and the substrate results in a high level of in-plane stress and defects (dislocations [5–10], stacking faults [8–10], twins [10], grain boundaries [9–11], micropipes [6, 8], point defects [8, 10, 12]) generation in the GaN epitaxial layer. The morphology of the GaN main epilayer

in GaN/sapphire heterostructures essentially depends both on the type of epilayer growth technology (molecular beam epitaxy (MBE) [1, 10, 12], chemical vapour deposition (CVD) [13], metal–organic CVD [9, 12], etc) and the parameters characterizing the buffer layer (compound, thickness, growth temperature and structural state [1]). In a series of works [1, 12, 14–19] the residual strains and stresses in the GaN epilayer have been investigated by high-resolution x-ray diffraction measurements. In the case of sapphire substrates, a high level of residual strains [1, 19] (of the order of  $10^{-3}$ ), stresses [1] (close to  $-0.9$  GPa) and mosaicity [11, 14, 16] (from a few to ten arcminutes) have been revealed for GaN epitaxial films grown by MBE.

The origin of stresses in GaN/sapphire heterostructures has been discussed in detail by Kisielowski [1]. It has been established that in GaN/sapphire heterostructures, for the given thicknesses of substrate and main epilayer, the stress in the GaN thin film can be manipulated by four main parameters: the buffer layer thickness; the buffer layer growth temperature; the compound parameter  $x$  of the Ga<sub>1-x</sub>N<sub>x</sub>

buffer layer; and doping. In this context, the investigations of strain and stress in the GaN epilayer depending on the compound parameter  $x$  are of special interest for the MBE technique, and until now have received little attention. In [20] it was demonstrated for the first time that the use of pure gallium (Ga) as a buffer layer results in the further improvement of the quality of the GaN epilayers. Plasma-assisted MBE on  $c$ -plane sapphire was used to grow Si-doped 2  $\mu\text{m}$  thick GaN epilayers after deposition of a thin Ga buffer layer. The resulting films typically show electron Hall mobility as high as  $\mu = 400 \text{ cm}^2 \text{ V}^{-1} \text{ s}^{-1}$ , which represents an outstanding value for a GaN layer grown by MBE on sapphire. Also, the structural properties are significantly improved; the asymmetric (10.1) x-ray rocking curve width (for the skew diffraction scheme of the Bragg set-up) is drastically reduced with respect to that of the reference GaN epilayer grown on the GaN buffer layer. It has been proposed that an increased stress relaxation by the soft gallium buffer layer during growth and/or cool-down is responsible for the improved material properties.

In this paper, we have carried out high-resolution x-ray diffraction strain–stress analysis of undoped GaN/Ga<sub>1-x</sub>N<sub>x</sub> buffer layer/(00.1)sapphire heterostructures depending on the compound parameter  $x$  of the buffer layer. As a special case, we have also investigated the deformation state of heterostructures with a buffer layer of pure Ga content.

## 2. Experiment

A series of GaN/sapphire heteroepitaxial structures were prepared by the plasma-assisted MBE technique. In these heteroepitaxial structures, an undoped GaN film with a thickness of 2  $\mu\text{m}$  was grown on a (00.1) sapphire substrate (with a thickness of 0.4 mm) with a thin GaN buffer layer (with a thickness of 4 nm). The GaN buffer layer and the GaN main layer deposition temperatures were equal to 800 K and 1000 K, respectively. During the growth of the buffer layer, the Ga source temperature was kept constant and the N flow rate was varied from sample to sample. As a result of this, the samples under investigation differ by the amount of nitrogen content in the Ga<sub>1-x</sub>N<sub>x</sub> buffer layer. Three samples were examined, numbered 1, 3 and 5 and prepared for the N flow rates 35, 15 and 0 sccm, respectively. By means of Auger electron spectroscopy measurements for the compound parameter  $x$ , the values of 0.394, 0.377 and 0 have been obtained for samples 1, 3 and 5, respectively. Motivation for the choice of growth parameters (growth temperature, buffer layer thickness) is described in detail in [1, 12].

For x-ray diffraction measurements, a high-resolution x-ray diffractometer, Siemens D-5000 equipped with a four-bounce Ge monochromator and four-circle translational capability, was employed. The double-axis CuK $\alpha_1$   $\theta - 2\theta$  x-ray diffraction spectra were recorded from GaN/sapphire structures for precise measurements of the  $c$ - and  $a$ -lattice parameters. In figure 1, only the  $\theta - 2\theta$  x-ray diffraction spectrum recorded from sample 3 is presented, since this result is representative.

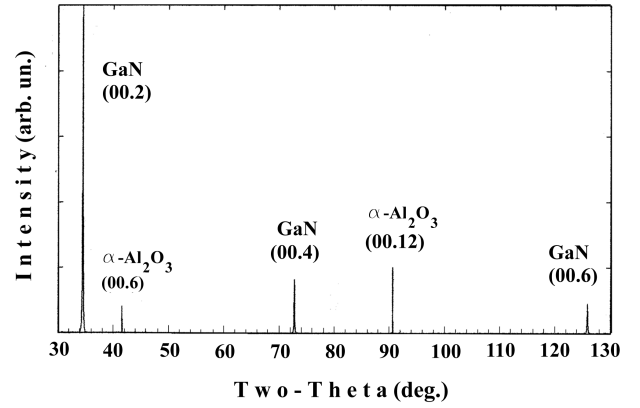


**Figure 1.** The x-ray diffraction  $\theta - 2\theta$  CuK $\alpha_1$  spectrum from the GaN/ $\alpha$ -Al<sub>2</sub>O<sub>3</sub> heteroepitaxial structure (sample 3).

## 3. Analysis of experimental results

### 3.1. Determination of out-of-plane and in-plane strain components in GaN films

The crystallographic structure of GaN belongs to the hexagonal space group. Besides, it is known [1, 9, 10] that a GaN film deposited on a (00.1) sapphire substrate is of a columnar structure. The axes of the columns, which are of hexagonal shape, coincide with the crystallographic  $c$ -axis of GaN and these columns are textured about the [00.1] crystallographic direction of the sapphire substrate with an effective angle of about a few arcminutes. Therefore, the  $a$  and  $b$  crystallographic axes of these columns are oriented practically parallel to the (00.1) plane of the substrate. For this reason, the GaN epilayer exhibits in-plane isotropic elastic properties, and its in-plane deformation state can be described by one strain component. Therefore, out-of-plane,  $\epsilon_c$ , and in-plane,  $\epsilon_a$ , strain components of the GaN film can be expressed as

$$\epsilon_c = \frac{c_r - c_0}{c_0} \quad (1)$$

and

$$\epsilon_a = \frac{a_r - a_0}{a_0} \quad (2)$$

where  $c_0$  and  $c_r$  are the unstrained and real (strained)  $c$ -lattice parameters, respectively, and  $a_0$  and  $a_r$  are the unstrained and strained  $a$ -lattice parameters, respectively.

The  $c$ -lattice parameter of GaN films was determined from  $\theta - 2\theta$  diffraction spectra detected for the Bragg symmetrical set-up. The spectra contain three diffraction peaks, (00.2), (00.4) and (00.6), recorded from the GaN main epilayer (figure 1). The data of the angular absolute positions of GaN (00. $h$ ) diffraction peaks ( $h = 2, 4, 6$ ;  $h$  is the order of reflection) are used for this measurement applying the well-known standard extrapolating technique [21]. The real value,  $c_r$ , of the  $c$ -lattice parameter and its experimental values,  $\{c_h\}$ , are connected through the angular parameter,  $p_h$ , by the relationship

$$c_h = -\frac{Dc_r}{r} p_h + c_r \quad (3)$$

where

$$p_h = \frac{\cos^2 \theta_h^{(e)}}{\sin \theta_h^{(e)}} \quad (4)$$

$$c_h = \frac{h\lambda}{2 \sin \theta_h^{(e)}}. \quad (5)$$

$\theta_h^{(e)}$  is the angular position of the GaN (00.*h*) diffraction peak in  $\theta$ -scale,  $c_h$  is the value of the *c*-lattice parameter determined from the angular position of the (00.*h*) diffraction peak,  $r$  is the distance specimen detector,  $D$  is a possible displacement of the specimen with respect to the goniometer axis in the equatorial plane, and  $\lambda$  is the wavelength of x-ray radiation. The lattice parameter  $c_r$  is determined from the plots  $\{p_h, c_h\}$  ( $h = 2, 4, 6$ ). Because of the high level of collimation of the incident x-ray beam ( $\approx 0.0033^\circ$ ) and the small thickness of the GaN epilayer, the instrumental aberrations caused both by the incident x-ray beam divergence (in equatorial and axial planes) and the finite absorption of x-rays were neglected. Therefore, in equation (3) only the instrumental aberration caused by the specimen misalignment is taken into account. For each sample, the lattice parameter  $c_r$  was determined for the four different azimuthal positions (each azimuthal position is achieved by a rotation of the sample about the *z*-axis through  $90^\circ$ ). In table 1 only one set  $\{\theta_h^{(e)}\}$  ( $h = 2, 4, 6$ );  $c_r$  of data corresponding to a certain azimuthal position is presented along with the relevant average value  $\bar{c}_r$  (averaging over the azimuthal positions). Finally, the out-of-plane strain component,  $\varepsilon_c$ , is determined from equation (1) for the average value  $\bar{c}_r$  and the unstrained lattice parameter  $c_0 = 0.5185$  nm measured for the homoepitaxially grown GaN films [22] (the data are listed in table 3). In an analogous way, using the above-mentioned method, from the plots

$$\left\{ p_{hkl} = \frac{\cos^2 \theta_{hkl}^{(e)}}{\sin \theta_{hkl}^{(e)}}, \quad a^{(hkl)} = cd_{hkl} \sqrt{\frac{(4/3)(h^2 + k^2 + hk)}{c^2 - l^2 d_{hkl}^2}} \right\} \quad (6)$$

for diffraction peaks of the asymmetrical reflections (*hkl.l*) = (10.1), (10.2), (20.2), (10.3), (10.4), (10.5) and (20.4), the *a*-lattice parameter of the GaN film was determined. For the reflections (10.1), (10.2), (20.2) and (10.3) the Bragg angle is smaller than the relevant angle between the reflecting atomic planes and the surface (00.1) plane. Therefore, for the detection of these reflections, the skew diffraction scheme for the Bragg set-up was used. In expression (6),  $d_{hkl}$  is the interplanar distance of (*hkl.l*) reflecting atomic planes determined from the  $\theta_{hkl}^{(e)}$  angular position of the relevant diffraction peak and  $c \equiv \bar{c}_r$ . The determined values for the *a*-lattice parameter and in-plane strain are presented in table 2. When calculating the in-plane strain from equation (2), the value  $a_0 = 0.31878$  nm [22] for the unstrained *a*-lattice parameter was used.

### 3.2. Separation of the biaxial and the hydrostatic strains from the measured strain

In the previous section, we have described the procedure of x-ray diffraction measurements both of out-of-plane,  $\varepsilon_c$ , and in-plane,  $\varepsilon_a$ , strains in the GaN main epilayer. However, it is known [1, 12] that the main GaN layer of heteroepitaxial GaN/sapphire structures grown by the MBE method contains a high concentration of point defects which cause a considerable contraction or expansion (depending on the concentration level and type of point defects) of the crystal lattice in this layer.

Therefore, out-of-plane and in-plane strain components in the GaN layer are the superposition of biaxial and hydrostatic strains [12]

$$\varepsilon_c = \varepsilon_c^{(b)} + \varepsilon_h \quad (7)$$

$$\varepsilon_a = \varepsilon_a^{(b)} + \varepsilon_h \quad (8)$$

where

$$\varepsilon_h = \frac{1 - \nu}{1 + \nu} \left( \varepsilon_c + \frac{2\nu}{1 - \nu} \varepsilon_a \right) \quad (9)$$

$$\nu = \frac{c_{13}}{c_{13} + c_{33}}. \quad (10)$$

In (7) and (8)  $\varepsilon_h$  is the hydrostatic strain,  $\varepsilon_c^{(b)}$  and  $\varepsilon_a^{(b)}$  are the biaxial strains in the *c*- and *a*-direction, respectively. In (9) and (10),  $\nu$  is the Poisson ratio, and  $c_{13}$  and  $c_{33}$  are the elastic constants of GaN. From the relevant theoretical calculations and the analysis performed by Wright [24], it follows that for GaN elastic constants  $c_{13}$  and  $c_{33}$  the most reliable values have been obtained by Brillouin scattering measurements [25] ( $c_{13} = 106$  GPa,  $c_{33} = 398$  GPa). After the substitutions of the data for these elastic constants into (10) and the measured strains  $\varepsilon_c$  and  $\varepsilon_a$  into (7)–(9), the out-of-plane (in the *c*-direction) and in-plane (in the *a*-direction) biaxial strain components,  $\varepsilon_c^{(b)}$  and  $\varepsilon_a^{(b)}$ , and the hydrostatic strain,  $\varepsilon_h$ , can be found from the set of simultaneous equations (7)–(10). The obtained results are listed in table 3.

### 3.3. Determination of biaxial stress in GaN films

The stresses in the heteroepitaxial films are biaxial by nature. It is established that in GaN/sapphire heterostructures the character of the stress originating from the mismatch between the epilayer and the substrate lattice parameters is really biaxial [1, 5, 12, 23]. The in-plane biaxial stress in the GaN epilayer can be determined from the relationships

$$\sigma_f = M_f \varepsilon_a^{(b)} \quad (11)$$

where

$$M_f = c_{11} + c_{12} - 2 \frac{c_{13}^2}{c_{33}}. \quad (12)$$

$\sigma_f$  is the biaxial stress in film,  $M_f$  is the biaxial elastic modulus for a material with a hexagonal structure strained about the [0001] crystallographic direction,  $c_{ij}$  are the elastic constants of GaN ( $c_{11} = 390$  GPa,  $c_{12} = 145$  GPa,  $c_{13} = 106$  GPa,  $c_{33} = 398$  GPa) [25]. Using these data for  $c_{ij}$ , the value  $M_f = 478.5$  GPa is obtained from (12) for the biaxial elastic modulus. The biaxial stress in film can be calculated from (11), substituting the values of biaxial strain in the *a*-direction and the elastic modulus. The biaxial stress component in the crystallographic *b*-direction equals the component in the *a*-direction, whereas the biaxial stress component in the *c*-direction equals zero. The data for  $\sigma_f$  are listed in table 3.

## 4. Discussion

In the GaN main epilayers, both the measured (i.e. total) and the biaxial out-of-plane strains are of tensile type, whereas both the measured and the biaxial in-plane strains are of compressive type. The maximal level for biaxial strain and stress is determined for sample 3 (compound parameter of

**Table 1.** The values of  $c_r$  (measured for a certain azimuthal position of the sample) and  $\bar{c}_r$  in the GaN main epilayer.

Sample	Diffraction peak position, $\theta_h^{(e)}$ (°) Order of reflection			Measured $c$ -lattice parameter $c$ (nm)	
	$h = 2$	$h = 4$	$h = 6$	$c_r$	$\bar{c}_r$
1	$17.303 \pm 0.002$	36.465	63.035	$0.51860 \pm 0.00002$	0.51857
3	17.162	36.325	62.857	0.51910	0.51910
5	17.274	36.436	62.984	0.51875	0.51882

**Table 2.** The value of the  $a$ -lattice parameter in the GaN main epilayer.

Sample	Diffraction peak position, $\theta_{hkl}^{(e)}$ (°) Reflection ( $hkl$ )							Measured $a$ -lattice parameter $a$ (nm)
	(10.1)	(10.2)	(10.3)	(20.2)	(10.4)	(10.5)	(20.4)	
1	$18.367 \pm 0.002$	24.123	31.724	39.221	41.087	52.479	54.659	$0.31801 \pm 0.00002$
3	18.539	24.138	31.714	39.249	41.049	52.488	54.681	0.31781
5	18.391	24.063	31.719	39.239	41.020	52.489	54.584	0.31810

**Table 3.** Strains and biaxial stress in GaN film of GaN/sapphire heteroepitaxial structures.

Sample	N content in buffer layer $x$ (%)	Measured strain in $c$ -direction $\varepsilon_c$	Measured strain in $a$ -direction $\varepsilon_a$	Hydrostatic strain $\varepsilon_h$	Biaxial strain in $c$ -direction $\varepsilon_c^b$	Biaxial strain in $a$ -direction $\varepsilon_a^b$	Biaxial stress $\sigma_f$ (GPa)
1	39.4	$1.35 \times 10^{-4}$ $\pm 4 \times 10^{-5}$	$-2.42 \times 10^{-3}$ $\pm 6 \times 10^{-5}$	$-7.51 \times 10^{-4}$ $\pm 1 \times 10^{-4}$	$8.86 \times 10^{-4}$ $\pm 1.4 \times 10^{-4}$	$-1.66 \times 10^{-3}$ $\pm 1.6 \times 10^{-4}$	$-0.79 \pm 0.04$
3	37.7	$1.16 \times 10^{-3}$	$-3.04 \times 10^{-3}$	$-3.03 \times 10^{-4}$	$1.46 \times 10^{-3}$	$-2.74 \times 10^{-3}$	-1.31
5	0	$6.17 \times 10^{-4}$	$-2.13 \times 10^{-3}$	$-3.39 \times 10^{-4}$	$9.56 \times 10^{-4}$	$-1.79 \times 10^{-3}$	-0.86

Lattice parameters for unstrained GaN [22]:  $a_0 = 0.31878 \pm 0.00003$  nm;  $c_0 = 0.51850 \pm 0.00002$  nm.

buffer layer  $x = 0.377$ ). As can be seen from the data of strains presented in table 3, the deformation state of a GaN/sapphire heterostructure essentially depends on the compound of the GaN buffer layer. This result is not unexpected if we take into account that, because of the large difference in the covalent radii of the Ga and the N atoms ( $r_{\text{Ga}} = 0.126$  nm,  $r_{\text{N}} = 0.07$  nm), the average in-plane interatomic distance in the  $\text{Ga}_{1-x}\text{N}_x$  buffer layer (a partial or full amorphization of the buffer layer is not excluded, therefore we intentionally avoid using the term ‘lattice parameter’ for the buffer layer),  $\bar{a}_b(x)$ , should considerably depend on the compound parameter  $x$ . In turn, the mismatch between the parameter  $\bar{a}_b(x)$  of the buffer layer and the in-plane lattice parameter  $a_f$  of the film, along with the mismatch between the parameter  $\bar{a}_b(x)$  of the buffer layer and the in-plane lattice parameter  $a_s$  of the substrate, to a certain degree control the deformation state of the heteroepitaxial structure. Thus, on the whole, we suppose that the worst effective matching at the substrate–buffer layer and buffer layer–film interfaces between atomic positions is achieved for sample 3.

It is interesting that the smallest value of the total (see equation (7)) in-plane strain in the film is determined for sample 5 with a buffer layer of pure Ga. There is a certain correlation between this result and the maximal stress relaxation degree determined for Si-doped films with pure Ga buffer layers in [20].

In general, it can be expected that the effective hydrostatic strain in GaN originates from  $N_{\text{Ga}}$  and  $Ga_{\text{N}}$  substitutional type point defects,  $N_i$  and  $Ga_i$  interstitial point defects, and  $V_{\text{N}}$  and

$V_{\text{Ga}}$  vacancies. As was mentioned above, the covalent radius of the Ga atom is considerably larger than the covalent radius of the N atom. Therefore,  $Ga_{\text{N}}$ ,  $Ga_i$  and  $N_i$  type defects cause a crystal lattice expansion, whereas  $N_{\text{Ga}}$ ,  $V_{\text{Ga}}$  and  $V_{\text{N}}$  type point defects lead to a crystal lattice compression. In our case, we find that for all samples the hydrostatic strain in GaN films is of compressive character and large by absolute value (see table 3). Therefore, we suppose that in the films the relative concentrations of  $N_{\text{Ga}}$ ,  $V_{\text{Ga}}$  and  $V_{\text{N}}$  type defects are dominant with respect to other types of point defects. However, in order to extract a contribution of each type of point defect from the total (measured) hydrostatic strain, it is necessary to perform an additional investigation. The smallest absolute value of hydrostatic strain is determined for sample 3, which exhibits, on the whole, extreme deformation behaviour. It could be supposed that in comparison with other samples, for sample 3, the parameter  $\bar{a}_b(x)$  of its  $\text{Ga}_{1-x}\text{N}_x$  buffer layer is closer to the in-plane lattice parameter of the GaN film. Therefore, for this sample, the most favourable conditions take place for coherent growth of the GaN main layer on the  $\text{Ga}_{1-x}\text{N}_x$  buffer layer leading to a comparatively small concentration of point defects and, hence, in compliance with Vegard’s law, to a comparatively low level of hydrostatic strain.

This is the first stage of our research and additional measurements by high-resolution TEM and atomic force microscopy will be conducted with the aim of studying the morphology of  $\text{Ga}_{1-x}\text{N}_x$  buffer layers (crystallinity and amorphism degree) and the growth mechanism of GaN films on buffer layers.

## Acknowledgments

The authors would like to thank Professor H-R Wenk for texture analysis of the samples, and Dr C Kisielowski and Dr Z Liliental-Weber for valuable discussions.

## References

- [1] Kisielowski C 1999 *Semicond. Semimet.* **57** 275
- [2] Nakamura S, Senoh M, Iwasa N and Nagahama S 1995 *Japan. J. Appl. Phys.* **34** L797
- [3] Kahn M A, Bhattarai A, Kuznia J N and Olsen D T 1993 *Appl. Phys. Lett.* **63** 1214
- [4] Nakamura S, Senoh M, Nagahama S, Iwasa N, Yamada T, Matsushita T, Kiyoku H and Sugimoto Y 1996 *Japan. J. Appl. Phys.* **35** L217
- [5] Perry W G, Zheleva T, Bremser M D, Davis R F, Shan W and Song J J 1997 *J. Electron. Mater.* **26** 224
- [6] Ruvimov S, Liliental-Weber Z, Suski T, Ager III J W, Washburn J, Kruger J, Kisielowski C, Weber E R, Amano H and Akasaki I 1996 *Appl. Phys. Lett.* **69** 12
- [7] Kisielowski C, Liliental-Weber Z and Nakamura S 1997 *Japan. J. Appl. Phys.* **36** 6932
- [8] Hwang C-Y, Schurman M J, Mayo W E, Lu Y-C, Stall R A and Salagaj T 1997 *J. Electron. Mater.* **26** 243
- [9] Ponce F A 1997 *MRS Bull.* (February) 51
- [10] Liliental-Weber Z, Sohn H, Newman N and Washburn J 1995 *J. Vac. Sci. Technol. B* **13** 1578
- [11] Hersee S D, Ramer J C and Malloy K J 1997 *MRS Bull.* (July) 45
- [12] Kisielowski C, Kruger J, Ruvimov S, Suski T, Ager III J W, Jones E, Liliental-Weber Z, Rubin M, Weber E R, Bremser M D and Davis R F 1996 *Phys. Rev. B* **54** 17 745
- [13] Zembutsu S and Sasaki T 1975 *Appl. Phys. Lett.* **48** 870
- [14] Saxler A, Capano M A, Mitchel W C, Kung P, Zhang X, Walker D and Razeghi M 1997 *Mater. Res. Soc. Symp. Proc.* **449** 447
- [15] Lafford T, Loxley N and Tanner B K 1997 *Mater. Res. Soc. Symp. Proc.* **449** 483
- [16] Goorsky, M S, Polyakov A Y, Skowronski M, Shin M and Greve D W 1997 *Mater. Res. Soc. Symp. Proc.* **449** 489
- [17] Duan S, Teng X, Li Y, Wang Y, Han P and Lu D 1997 *Mater. Res. Soc. Symp. Proc.* **468** 207
- [18] Le Vaillant Y-M, Clur S, Andenet A, Briot O, Gil B, Aulombard R L, Bisaro R, Olivier J, Durand O and Duboz J-Y 1997 *Mater. Res. Soc. Symp. Proc.* **468** 173
- [19] Harutyunyan V S, Monteiro P J M and Weber E R 2001 *Phys. Status Solidi A* submitted
- [20] Kim Y, Subramanya S G, Siegle H, Krueger J and Weber E R 2000 *Abstracts of Mater. Res. Soc. Meeting (April, 2000, San Francisco, USA)* p 318
- [21] Umanskii Y S, Skakov Y A, Ivanov A N and Rastorguyev L N 1982 *Crystallography, Rentgenography and Electron Microscopy* (Moscow: Metalurgiya)
- [22] Leszczynski M, Teisseyre H, Suski T, Grzegory I, Bockowski M, Jun J, Porowski S, Pakula K and Baranowski J M 1998 private communication
- [23] Skromme B J, Zhao H, Wang D, Kong H S, Leonard M T, Bulman G E and Molnar R J 1997 *Appl. Phys. Lett.* **71** 829
- [24] Wright A F 1997 *J. Appl. Phys.* **82** 2833
- [25] Polian A, Grimsditch M and Grzegory I G 1996 *J. Appl. Phys.* **79** 3343